PLOS | ONE

RESEARCH ARTICLE

Baseline Assessment of Net Calcium Carbonate Accretion Rates on U.S. Pacific Reefs

Bernardo Vargas-Ángel[1]*, Cristi L. Richards[2], Peter S. Vroom[3], Nichole N. Price[4], Tom Schils[5], Charles W. Young[1], Jennifer Smith[6], Maggie D. Johnson[6], Russell E. Brainard[7]

1 Joint Institute for Marine and Atmospheric Research, University of Hawaii, Honolulu, Hawaii, 96818, United States of America, **2** 2525 Date St. Apt. 3101, Honolulu, Hawaii, 96826–5420, United States of America, **3** Ocean Associates, 1846 Wasp Blvd. Bldg., # 176, Honolulu, Hawaii, 96818, United States of America, **4** Bigelow Laboratory for Ocean Sciences, 60 Bigelow Dr., East Boothbay, Maine, 04544, United States of America, **5** University of Guam Marine Laboratory, Mangilao, Guam, 96913, United States of America, **6** Scripps Institution of Oceanography, University of California San Diego, 9500 Gilman Dr., La Jolla, California, 92093, United States of America, **7** NOAA Pacific Islands Fisheries Science Center, Coral Reef Ecosystem Division, 1846 Wasp Blvd. Bldg. # 176, Honolulu, Hawaii, 96818, United States of America

* Bernado.VargasAngel@noaa.gov

OPEN ACCESS

Citation: Vargas-Ángel B, Richards CL, Vroom PS, Price NN, Schils T, Young CW, et al. (2015) Baseline Assessment of Net Calcium Carbonate Accretion Rates on U.S. Pacific Reefs. PLoS ONE 10(12): e0142196. doi:10.1371/journal.pone.0142196

Editor: Christian R Voolstra, King Abdullah University of Science and Technology, SAUDI ARABIA

Received: March 10, 2015

Accepted: October 18, 2015

Published: December 7, 2015

Data Availability Statement: All relevant data are within the paper; any additional data requests may be directed to: http://www.pifsc.noaa.gov/cred/data_portal.php.

Funding: This work was supported by the NOAA Coral Reef Conservation Program, the NOAA NMFS Office of Science and Technology, and NOAA Ocean Acidification Program. Institutional, logistic, and financial support was also provided by NOAA Pacific Islands Fisheries Science Center's Coral Reef Ecosystem Division (CRED) and Scripps Institution of Oceanography. The funders had no role in study design, data collection and analysis, decision to

Abstract

This paper presents a comprehensive quantitative baseline assessment of *in situ* net calcium carbonate accretion rates (g $CaCO_3$ cm^{-2} yr^{-1}) of early successional recruitment communities on Calcification Accretion Unit (CAU) plates deployed on coral reefs at 78 discrete sites, across 11 islands in the central and south Pacific Oceans. Accretion rates varied substantially within and between islands, reef zones, levels of wave exposure, and island geomorphology. For forereef sites, mean accretion rates were the highest at Rose Atoll, Jarvis, and Swains Islands, and the lowest at Johnston Atoll and Tutuila. A comparison between reef zones showed higher accretion rates on forereefs compared to lagoon sites; mean accretion rates were also higher on windward than leeward sites but only for a subset of islands. High levels of spatial variability in net carbonate accretion rates reported herein draw attention to the heterogeneity of the community assemblages. Percent cover of key early successional taxa on CAU plates did not reflect that of the mature communities present on surrounding benthos, possibly due to the short deployment period (2 years) of the experimental units. Yet, net $CaCO_3$ accretion rates were positively correlated with crustose coralline algae (CCA) percent cover on the surrounding benthos and on the CAU plates, which on average represented >70% of the accreted material. For foreeefs and lagoon sites combined $CaCO_3$ accretion rates were statistically correlated with total alkalinity and Chlorophyll-a; a GAM analysis indicated that SiOH and *Halimeda* were the best predictor variables of accretion rates on lagoon sites, and total alkalinity and Chlorophyll-a for forereef sites, demonstrating the utility of CAUs as a tool to monitor changes in reef accretion rates as they relate to ocean acidification. This study underscores the pivotal role CCA play as a key benthic component and supporting actively calcifying reefs; high Mg-calcite exoskeletons makes CCA extremely susceptible changes in ocean water pH, emphasizing the far-

publish, or preparation of the manuscript. Ocean Associates provided support in the form of a salary for author PSV, but did not have any additional role in the study.

Competing Interests: Peter S. Vroom was employed by Ocean Associates at the time of manuscript preparation. There are no patents, products in development or marketed products to declare. This did not alter the authors' adherence to all the PLOS ONE policies on sharing data and materials, as detailed online in the guide for authors.

reaching threat that ocean acidification poses to the ecological function and persistence of coral reefs worldwide.

Introduction

The uptake of atmospheric carbon dioxide (CO_2) by seawater and subsequent equilibrium reactions within this ionic medium are part of the complex chemical system often referred to as the marine carbonate system. As atmospheric CO_2 dissolves in seawater, it forms the weak carbonic acid (H_2CO_3), which in turn dissociates into bicarbonate (HCO_3^-) and carbonate (CO_3^{2-}) ions, and the associated protons (H^+). Natural processes including gas exchange, photosynthesis, respiration, calcium carbonate ($CaCO_3$) precipitation, and dissolution, influence the distribution of chemical species of the carbonate system as a function of pH [1]. With increased uptake of atmospheric CO_2 by the ocean, the pH decreases together with CO_3^{2-} and $CaCO_3$ saturation state of seawater, while HCO_3^- increases [2]. However, because the ocean stores roughly 60 times more inorganic carbon than the atmosphere [3], even small changes in the components of the marine carbonate system can have far-reaching implications for surface ocean chemistry, physical properties, individual marine organisms, and marine ecosystems [1, 4, 5].

Since the beginning of the Industrial Revolution, atmospheric global CO_2 levels have risen by nearly 40% mainly due to the burning of fossil fuels, deforestation, and changes in land usage [6, 7, 8]. It is estimated that elevated CO_2 concentrations have caused ocean waters to decrease in pH by 0.11 units [9] through the process termed ocean acidification (OA). It is projected that if CO_2 emissions continue at current rates, atmospheric CO_2 will reach twice pre-industrial levels by 2065 [10, 11, 12] and ocean surface water pH decrease by 0.14–0.35 units by 2100 [13, 9]. This projected change in ocean water chemistry reduces the pH and the aragonite and calcite ($CaCO_3$) saturation states, approaching levels that may not support biogenic calcification but instead drive net dissolution of marine carbonate structures [14, 15, 16, 17]. In addition to calcification, the adverse effects of OA to marine organisms are multiple, affecting other biological and physiological processes, including reproduction, recruitment, development, and growth [18, 19, 20, 21], photosynthesis and respiration [22, 23], acid-base balance and oxygen transport capacity [24,25], behavior, and tolerance to secondary disturbances [26, 27,28].

In shallow tropical marine ecosystems, corals, coralline algae, and other calcifying organisms are responsible for the accretion of biogenic $CaCO_3$ that creates the massive, three-dimensional edifices that define coral reef ecosystems and provide the habitat that supports high marine biodiversity. As one of projected consequences of OA to shallow tropical coral reefs, decreased calcification affects carbonate production and consequently net reef accretion rates, potentially impairing ecosystem functionality [29, 30], making coral reefs among the most susceptible marine ecosystems to environmental conditions that impact calcification and/or promote dissolution of $CaCO_3$ [31]. Interestingly, the direction and magnitude of the effects appear to be species specific [32, 33].

Calcifying marine macroalgae are a principal component of the carbonate budget on coral reefs, and recent studies suggest they are extremely susceptible to chemical changes associated with OA [16]. Lee and Carpenter [34] estimated that ~50–55% of carbonates present in shallow, tropical marine systems are derived from corals and crustose coralline algae (CCA), while ~35–40% are derived from siphonous green algae (e.g., *Halimeda*, *Udotea*, *Penicillus*, *Rhipocephalus* [35, 36]), and the remaining ~10% are derived from other biogenic calcifiers such as

mollusks, echinoderms, and bryozoans [34]. CCA are key components of tropical reef ecosystems [37, 38], often recruiting immediately after disturbances [39] to cement, reinforce, and consolidate carbonate material, often serving as preferred settlement habitat for coral recruits [40, 41], thus, contributing to the buildup, maintenance, and temporal persistence of reef structures [42, 43, 44]. Moreover, species of CCA with skeletal mineralogy composed of high Mg-calcite content are more soluble than organisms with aragonite (corals, *Halimeda*) or calcite (mollusks), and therefore may be the first to be impacted by OA through increased dissolution [45, 46]. In addition, although species-specific, it appears that the extent of damage caused by low pH conditions also depends on the rate of change in the carbonate chemistry [47, 48].

To date, most studies of *in situ* carbonate accretion rates are spatially discrete and conducted on reefs close to urban settlements that are subject to varying levels of anthropogenic impact. Although useful, these data limit our understanding of natural, large-scale spatial patterns, and variability in accretion rates, and fail to provide an accurate baseline that is suitable for modeling or predicting the future effects of OA. To bridge this critical gap, we present the first quantitative baseline of *in situ* net carbonate accretion rates from 78 reefs located on 11 islands in the central Pacific, ranging from high island locales in close proximity to human impacts, to quasi-pristine environs thousands of kilometers away from continental and human influence (see [49]), across various habitats (e.g., lagoons and forereefs), and exposure to wave activity. Using simple and easily-deployed Calcification Accretion Units (CAUs), this study documents and examines: (1) the spatial variation of *in situ* carbonate accretion rates throughout American Samoa and the Pacific Remote Islands Marine National Monument (PRIMNM), (2) the potential association with physical, biological, and oceanographic drivers, and (3) the relational context between observed accretion rates and the composition of the surrounding benthos.

Materials and Methods

Study area

Between February and April 2010, the Coral Reef Ecosystem Division (CRED) of the NOAA Pacific Islands Fisheries Science Center (PIFSC) deployed 390 CAUs at 78 reef sites, within two major biogeographical regions (central and south Pacific), including six islands/atolls in the Pacific Remote Islands Marine National Monument (PRIMNM; i.e., Howland, Baker, and Jarvis Islands, Johnston and Palmyra Atolls, and Kingman Reef); and five islands/atolls in American Samoa (i.e., Rose Atoll and Swains, Ta`u, Ofu-Olosega, and Tutuila Islands; Fig 1, Table 1). Study sites spanned ~1700 km E–W and ~3400 km N–S, across a diverse range of geomorphologies, from steep volcanic high islands (e.g., Tutuila, Ta`u, and Ofu-Olosega) to low carbonate islets and atolls (e.g., Howland, Baker, and Jarvis Islands). Oceanographic conditions ranged from intense equatorial and topographic upwelling at Jarvis Island to oligotrophic conditions at many islands (e.g., Rose and Johnston Atolls) [50]; and anthropogenic impact regimes ranged from fishing and chronic coastal runoff (e.g., Tutuila) to lack of any present-day direct human impacts (e.g., Howland and Baker islands, and Kingman Reef) [51].

Carbonate accretion and community structure

Each CAU assembly comprised two 10 cm × 10cm (100-cm^2) polyvinyl chloride (PVC) plates separated by a 1 cm plastic spacer and mounted on a stainless steel all-thread rod (Fig 2). Each PVC plate was sanded to provide a non-glossy surface suitable for permanent attachment and settlement of marine propagules. These assemblies were attached to stainless steel stakes installed into hard carbonate or basalt reef substrate at depths of 5.5–15 m at permanent CRED benthic, Rapid Ecological Assessment (REA) survey sites. Five CAUs were installed at each

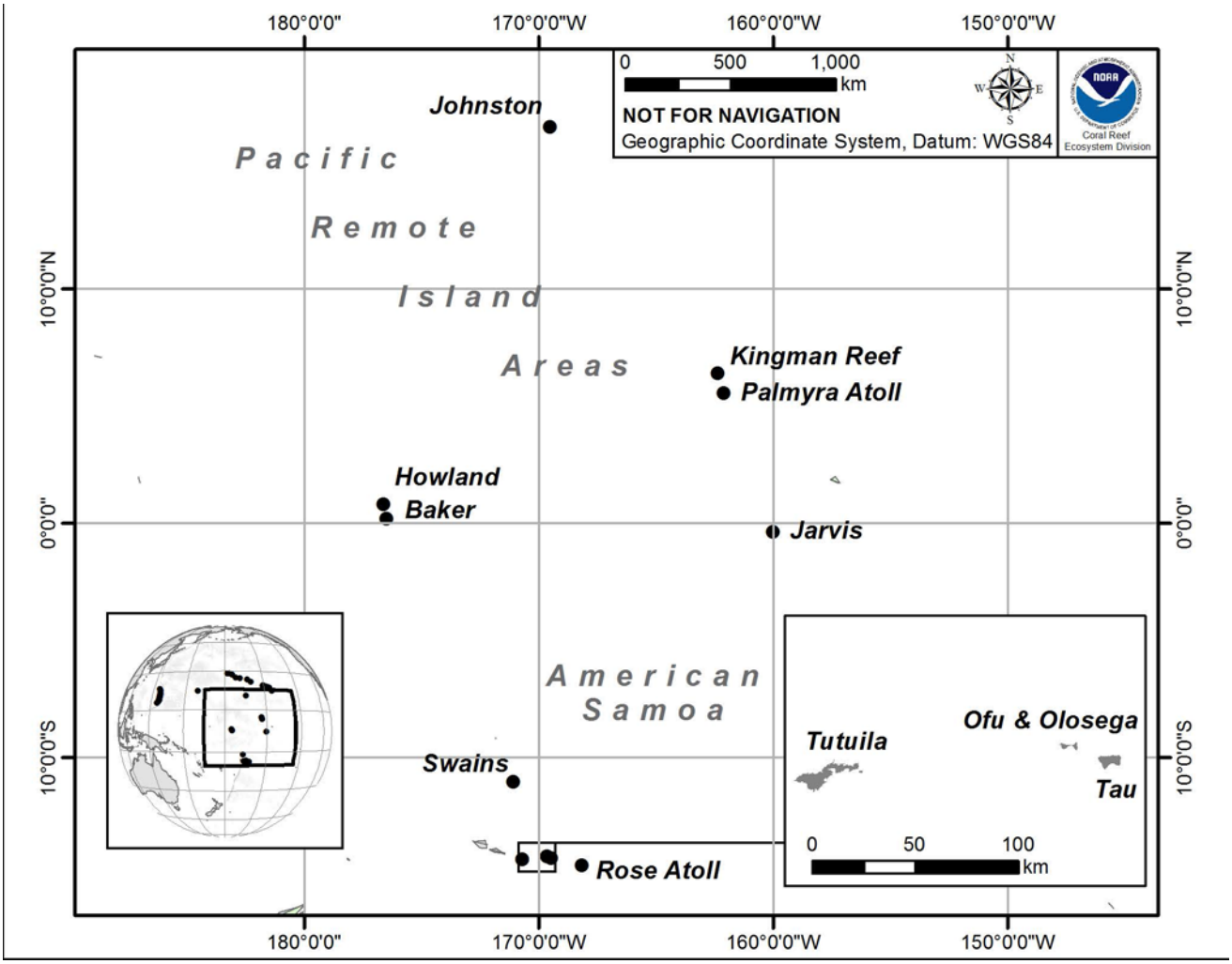

Fig 1. Geographical location of the U.S.-Affiliated Pacific Islands and Atolls where Calcification Accretion Units (CAUs) were deployed and recovered between 2010 and 2012.

doi:10.1371/journal.pone.0142196.g001

site, with each CAU being positioned approximately 10 cm above the substrate with a spacing of 0.5–3 m between each CAU. CAUs were typically installed at a minimum of 5 sites per island (2 islands/atolls had only four) and sites were spread out across the forereef and lagoon sites (where possible) for representative spatial coverage.

CAUs were deployed for a ~2-year period and were recovered during the February–May 2012 CRED-led Pacific Reef Assessment and Monitoring Program (Pacific RAMP) research cruise. During recovery, each CAU was placed in a Ziploc® bag to minimize the loss of attached organisms or calcified material during transport to the shipboard laboratory onboard the NOAA ship *Hi`alakai*. In this laboratory, CAUs were rinsed in salt water to remove mobile fauna and sediment/sand, and then frozen at –5°C for preservation during transportation to the laboratory in Honolulu (7–60 days). In the Honolulu laboratory, each CAU was disassembled and each plate submerged in a shallow (5 cm) basin of salt water; the upper and lower surfaces of both plates were photographed to characterize and quantify the settled early successional benthic community.

Table 1. Calcification Accretion Unit site locations, depth, reef zone, mean accretion rates, and standard deviation (SD). Availability of benthic cover data from Line-Point-Intercept (LPI) surveys is indicated, Y: yes; N: no.

Archipelago	Island/ Atoll	REA Site	Latitude	Longitude	Depth (m)	Reef zone	Mean accretion rate (g cm^{-2} yr^{-1})	SD	LPI
Pacific	**Baker**	BAK-02	0.18839	-176.47994	16.0	Forereef	0.045	0.010	Y
Remote		BAK-11	0.19918	-176.48454	10.5	Forereef	0.037	0.006	Y
Island		BAK-14	0.20509	-176.47457	16.0	Forereef	0.113	0.014	Y
Areas		BAK-16	0.19454	-176.46287	12.0	Forereef	0.092	0.041	Y
	Howland	HOW-05	0.80409	-176.62106	11.5	Forereef	0.072	0.017	Y
		HOW-11	0.79882	-176.62025	13.5	Forereef	0.070	0.015	Y
		HOW-12	0.80924	-176.61068	12.3	Forereef	0.069	0.021	N
		HOW-13	0.81962	-176.61619	12.2	Forereef	0.131	0.027	N
		HOW-14	0.81463	-176.62386	14.0	Forereef	0.068	0.008	Y
	Jarvis	JAR-01	-0.36787	-159.97919	15.5	Forereef	0.201	0.033	Y
		JAR-07	-0.37611	-160.01393	13.0	Forereef	0.061	0.019	Y
		JAR-08	-0.36314	-159.99139	13.5	Forereef	0.106	0.020	Y
		JAR-10	-0.38128	-159.97264	13.5	Forereef	0.077	0.050	Y
		JAR-11	-0.36902	-160.00819	13.0	Forereef	0.075	0.023	Y
	Johnston	JOH-09	16.72862	-169.48573	7.9	Lagoon	0.011	0.003	Y
		JOH-10	16.76337	-169.51201	14.4	Lagoon	0.006	0.002	Y
		JOH-11	16.72154	-169.52430	11.4	Lagoon	0.043	0.016	Y
		JOH-12	16.74766	-169.52396	11.0	Lagoon	0.016	0.004	Y
	Kingman	KIN-03	6.39029	-162.36066	11.0	Lagoon	0.064	0.006	Y
		KIN-04	6.43872	-162.38824	15.0	Forereef	0.115	0.019	Y
		KIN-05	6.39325	-162.34746	13.0	Lagoon	0.058	0.028	Y
		KIN-07	6.40219	-162.38522	10.0	Lagoon	0.112	0.025	Y
		KIN-10	6.42041	-162.37955	12.8	Lagoon	0.085	0.019	Y
		KIN-11	6.38196	-162.34638	13.5	Forereef	0.106	0.013	Y
		KIN-13	6.38220	-162.38406	12.0	Forereef	0.084	0.019	Y
		KIN-16	6.39240	-162.34210	7.0	Lagoon	0.055	0.030	Y
	Palmyra	PAL-01	5.86802	-162.06927	14.0	Forereef	0.048	0.021	Y
		PAL-05	5.89582	-162.13795	15.0	Forereef	0.110	0.029	Y
		PAL-11	5.88343	-162.13340	15.0	Forereef	0.061	0.008	Y
		PAL-12	5.89713	-162.10785	14.5	Forereef	0.059	0.013	Y
		PAL-19	5.86630	-162.10956	14.5	Forereef	0.109	0.019	Y
		PAL-21	5.89556	-162.08600	13.5	Forereef	0.039	0.009	Y
		PAL-25	5.86384	-162.03055	15.0	Forereef	0.078	0.004	Y
		PAL-26	5.86414	-162.12698	15.0	Forereef	0.086	0.019	Y
American	**Ofu-**	OFU-01	-14.16445	-169.65573	14.0	Forereef	0.115	0.023	Y
Samoa	**Olosega**	OFU-02	-14.18511	-169.67573	13.5	Forereef	0.101	0.029	Y
		OFU-03	-14.18649	-169.66021	14.5	Forereef	0.102	0.027	Y
		OFU-04	-14.17766	-169.64950	12.0	Forereef	0.098	0.017	Y
		OFU-06	-14.17419	-169.68197	13.5	Forereef	0.087	0.009	Y
		OFU-09	-14.15764	-169.67424	10.5	Forereef	0.079	0.015	Y
		OLO-01	-14.16854	-169.60783	14.5	Forereef	0.113	0.032	Y
		OLO-04	-14.18173	-169.62661	12.5	Forereef	0.099	0.024	Y
		OLO-05	-14.16343	-169.62465	11.0	Forereef	0.069	0.006	Y
	Rose	ROS-01	-14.53946	-168.14550	12.5	Forereef	0.152	0.019	Y
		ROS-03	-14.55480	-168.14655	13.5	Forereef	0.175	0.025	Y
		ROS-04	-14.55966	-168.15999	12.5	Forereef	0.189	0.023	Y

(*Continued*)

Table 1. (*Continued*)

Archipelago	Island/ Atoll	REA Site	Latitude	Longitude	Depth (m)	Reef zone	Mean accretion rate (g cm^{-2} yr^{-1})	SD	LPI
		ROS-06	-14.53641	-168.16548	14.5	Forereef	0.095	0.030	Y
		ROS-08	-14.53789	-168.15330	9.8	Lagoon	0.028	0.017	Y
		ROS-09	-14.55125	-168.16031	5.5	Lagoon	0.013	0.004	Y
		ROS-19	-14.54910	-168.13785	14.0	Forereef	0.181	0.042	Y
		ROS-23	-14.54216	-168.17235	13.5	Forereef	0.132	0.023	Y
		ROS-25	-14.52932	-168.15348	10.0	Forereef	0.132	0.034	Y
	Swains	SWA-01	-11.06832	-171.08118	15.0	Forereef	0.139	0.029	Y
		SWA-03	-11.05769	-171.09142	14.5	Forereef	0.089	0.020	Y
		SWA-07	-11.05098	-171.06581	15.5	Forereef	0.104	0.022	Y
		SWA-08	-11.04569	-171.07708	16.0	Forereef	0.076	0.035	Y
		SWA-16	-11.05074	-171.09223	12.5	Forereef	0.093	0.023	Y
	Tau	TAU-02	-14.25171	-169.44617	12.0	Forereef	0.082	0.012	Y
		TAU-04	-14.21240	-169.44066	12.5	Forereef	0.097	0.017	Y
		TAU-07	-14.22730	-169.41833	13.0	Forereef	0.094	0.010	Y
		TAU-08	-14.26240	-169.47480	13.5	Forereef	0.110	0.012	Y
		TAU-09	-14.24573	-169.50659	12.8	Forereef	0.100	0.021	Y
		TAU-11	-14.21723	-169.51281	14.5	Forereef	0.064	0.010	Y
		TAU-12	-14.25756	-169.50101	12.0	Forereef	0.072	0.008	Y
	Tutuila	TUT-01	-14.28354	-170.63782	13.0	Forereef	0.070	0.019	Y
		TUT-02	-14.27780	-170.60723	13.0	Forereef	0.048	0.006	Y
		TUT-05	-14.25169	-170.62309	15.0	Forereef	0.043	0.005	Y
		TUT-06	-14.32810	-170.83183	14.0	Forereef	0.056	0.011	Y
		TUT-08	-14.29167	-170.78042	15.0	Forereef	0.043	0.012	Y
		TUT-09	-14.33608	-170.70438	9.0	Forereef	0.069	0.020	Y
		TUT-10	-14.31101	-170.69303	14.0	Forereef	0.073	0.024	Y
		TUT-13	-14.26055	-170.71205	15.0	Forereef	0.053	0.008	Y
		TUT-14	-14.25334	-170.65219	14.5	Forereef	0.053	0.009	Y
		TUT-16	-14.28532	-170.56407	14.0	Forereef	0.058	0.014	Y
		TUT-17	-14.24600	-170.57196	13.5	Forereef	0.088	0.026	Y
		TUT-19	-14.28319	-170.72825	15.5	Forereef	0.050	0.011	Y
		TUT-22	-14.36588	-170.76284	14.0	Forereef	0.078	0.017	Y

doi:10.1371/journal.pone.0142196.t001

Subsequently, plates were dried at 60° C for 2–5 days, repeatedly weighed throughout the drying process, and classified as dry when the difference in weight between sequential weighings was less than 0.1g. After drying, each individual plate was submerged in 5% HCl for 24 hrs or until all $CaCO_3$ had dissolved. During the dissolution process, plates were periodically agitated (every 1–8 hrs) to reduce the boundary layer dissolution impediments, and large pieces of $CaCO_3$ were crushed using a pestle to speed dissolution. As the HCl solution was neutralized by the $CaCO_3$ dissolution (indicated by the absence of gas bubbles), additional HCl was added to complete the dissolution process. Often, the addition of acid was repeated several times in a 24–72 hr period until all $CaCO_3$ was removed. The remaining fleshy tissue was scraped onto pre-weighed 11 μm cellulose filter paper, vacuum filtered along with all 5% HCl supernatant from the dissolution process, dried at 60°C (until constant weight using the same dryness criteria above; 48 hours minimum), and weighed. Finally, the clean, scraped, and dried CAU plates were re-weighed, and the mass of $CaCO_3$ was determined by subtracting the combined weight of the fleshy tissue and PVC plates from the initial dry weight of the CAU prior to dissolution.

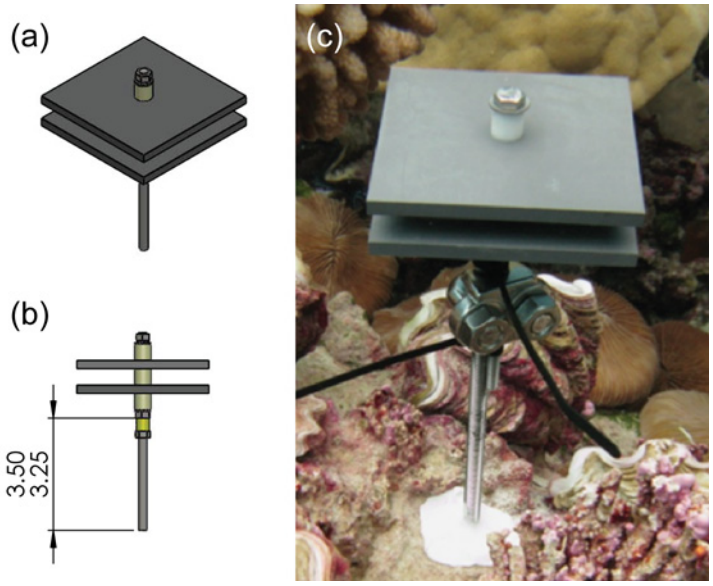

Fig 2. CAU assembly unit: a) oblique view, b) side view, and c) in-situ image of deployed CAU unit. (Photo and figure credit: Coral Reef Ecosystem Division, NOAA).

doi:10.1371/journal.pone.0142196.g002

To determine the rate of $CaCO_3$ accretion, the mass of $CaCO_3$ was normalized for surface area of each CAU (400 cm^2—accounting for all upper and lower plate surfaces) and the amount of time in days that each CAU was deployed, rendering a measure of net $CaCO_3$ accretion in units of g cm^{-2} yr^{-1}.

Community composition and percent cover of all taxa recruiting to and settling on the CAUs were characterized based on image analysis of each of the 4 CAU plate surfaces, implementing the software PhotoGrid 1.0 (25 stratified random points analyzed per surface). Sessile organisms were classified into ecological functional groups as follows: calcified macroinvertebrates, corals, crustose coralline algae (CCA) (i.e., Family Corallinaceae), encrusting macroalgae, *Halimeda* spp., calcified macroalgae, other calcified algal crusts (i.e., Family Peyssonneliaceae), algal turf assemblages, fleshy macroalgae, and macroinvertebrates (Table 2). For most of the taxa recruiting to and settling on the CAUs, the polymorph of $CaCO_3$ is known [52, 53, 54] (Table 2). Thus, based on image analysis of each CAU plate, the relative percent cover contribution for each $CaCO_3$ polymorph (aragonite, calcite, or high Mg-calcite) on the CAU plates was calculated by categorizing the calcifying taxa according to their mineralogy, following Price et al. 2010 [29].

Assessment of biotic parameters in the study sites

Percent benthic cover at each REA site was estimated implementing the Line-Point-Intercept (LPI) methodology at 20 cm intervals along two 25 m line transects set in a single file row (separated by 5 m) at the time of CAU recovery. Live benthic elements, including coral, macroalgae, and other sessile invertebrates were identified to the lowest taxonomic level possible. In addition, at the time of CAU retrieval, benthic communities surrounding each CAU site were photo-documented along the two 25 m transect lines (Table 1). A total of 32 digital images were taken at each site at an elevation of approximately 1 m from the surface of the substrate; these images provided a total sample area of 12 m^2. Each image was analyzed using Coral Point Count with Excel extensions (v. 4.12) image analysis software (10 stratified random points analyzed per image) [55]. Macroscopic taxa were identified to functional group following an analogous classification scheme as to that implemented for the taxa recruited onto the CAU plates

Table 2. Functional group classification and mineralogical exoskeletal composition of the taxa comprising the benthic communities at study sites and recruited to the CAU plates. NC: non-calcifying.

Functional group	Taxa	$CaCO_3$ skeleton mineralogy
Calcified invertebrate	Calcified tubeworms	Calcite
	Barnacle	Calcite
	Entoproct	Calcite
	Encrust/branched bryozoan	Calcite
	Vermetid, bivalve	Calcite/Aragonite
	Other calcified Invert	Calcite
CORAL	Scleractinian coral	Aragonite
	Hydrocoral	Aragonite
CCA	Encrusting coralline algae	High Mg-Calcite
	Branching coralline algae	High Mg-Calcite
Calcified algal crusts	*Palmophyllum*	Calcite
	Lobophora	Calcite
	Peyssonellia	Calcite
	Brown crust	Calcite
Halimeda	*Halimeda*	Aragonite
Calcified macroalgae	*Dictyota*	Calcite
	Calcified red macroalgae	Calcite
$CaCO_3$	Sediment	Calcite/Aragonite
	Calcium carbonate	Calcite
Fleshy macroalgae	Fleshy red r macroalgae	NC
	Fleshy green algae	NC
	Cyanophyte	NC
Turf	Sponge-turf matrix	NC
	Sediment-turf matrix	NC
	Mixed turf	NC
	Filamentous brown algae	NC
	Filamentous green algae	NC
	Filamentous red algae	NC
NON-CAL	Fleshy inverts	NC
	Colonial tunicate	NC
	Fleshy tubeworm	NC
	Solitary tunicate	NC
	Sponge	NC
	Small tubeworms	NC
	Egg mass	NC
	Biofilm	NC
	Other	NC

doi:10.1371/journal.pone.0142196.t002

(Table 2). Based on this image analysis, the relative percent cover contribution of each $CaCO_3$ polymorph (aragonite, calcite, or high-Mg calcite) of the reef benthos was also calculated by categorizing the calcifying taxa according to their mineralogy [29].

Assessment of abiotic parameters: water sampling

Discrete water samples were collected by SCUBA divers using a 5 L Niskin bottle directly above the benthos at each REA site during recovery of the CAUs. Thus, water was collected at

the depth of the CAU deployment sites. In concert with the water collection, a Seabird 19plus conductivity-temperature-depth (CTD) hydrocast was conducted to characterize the water salinity above the CAU deployment site at the time of discrete water sample collection. Upon completion of the CAU recovery/water sample dive, one 500 ml water subsample from the Niskin bottle was immediately collected and preserved for analysis of total dissolved inorganic carbon, total alkalinity, salinity, dissolved inorganic nutrients, and chlorophyll-*a*. Water samples were stored onboard the NOAA Ship *Hi'ialakai*, following established published techniques [56], and were analyzed at various NOAA and academic institutions within 7 to 60 days following the completion of Pacific RAMP research cruise (Table 3).

Data analysis

Spatial patterns of mean accretion rates were tested using several independent ANOVA models. A more comprehensive model was not possible because the sample size among the different levels within factors was unbalanced, precluding the analysis of 3-way interactions. Thus, two-way ANOVAs tested for the interaction between island (n = 11) and reef zone (forereef vs. lagoon), island and wave exposure (leeward vs. windward), and wave exposure and island geomorphology (volcanic vs. carbonate) as factors. Data were square root-transformed to fulfill parametric statistical requirements. The tests of island and wave exposure, and wave exposure and island geomorphology, were run on forereef data only. Additional non-parametric Kruskal-Wallis ANOVAs were implemented to test for differences in percent cover of calcifying taxa between the CAU plates and the benthos, and for spatial differences in percent cover of CCA and macroalgae+turf algae of the CAU plates; pair-wise comparisons (Dunn's test) were performed to establish differences among islands. Due to the constrains placed by the assumptions of parametric statistics, Spearman Rank Order Correlation tests were implemented to explore the association between: 1) the percent cover of CCA on the CAU plates vs. the benthos; 2) the site-specific mean accretion rates and the percent cover of CCA on the CAU plates; and 3) island mean accretion rates and water chemistry parameters. All ANOVA and correlation analyses above mentioned were performed using SYSTAT 12 version 12.02.00 [57].

To further explore the combined effects of the biotic and abiotic parameters a Regression with Empirical Variable Selection Procedure (hereafter REVS) was employed to identify models that best predicted the spatial variability in carbonate accretion rates across reefs in the study area. The REVS procedure evaluates all possible regression models (i.e., combination of predictor variables) and displays the best-fitting models that contain one predictor, two predictors, and so on [58]. Because differences in the benthic communities between forereef and lagoon habitats can have an important effects on calcium carbonate accretion mechanisms and rates; lagoon sites (n = 11) and forereef sites (n = 67) were analyzed separately. Two sets of predictor variables were evaluated to investigate relationships with carbonate accretion rates: (1) biotic; i.e, the percent cover of benthic organisms in the benthic transect survey dataset and (2) abiotic; i.e, water quality parameters The relationship between the remaining predictor variables for each set, and carbonate accretion rates were then analyzed using Generalized Additive Models (GAM). All carbonate accretion rate analyses were performed in R (R Development Core Team, 2014) using the packages "agricolae", "car", "doBy", "leaps", "MASS", "mgcv", "pgirmess", "plyr", "reshape", "stringr" as well as the non-packaged R function "REVS" [58].

Finally, to determine the similarity between the overall percent cover of the organisms on CAU plates and the overall percent cover of the organisms on the benthos, a RELATE test was conducted using PRIMER v.6. This test performs a series of non-parametric correlations between all elements within each of the two data sets. If the among-sample relationships agree in exactly the same way in both data sets, then the overall rank correlation rho-value (ρ) = 1,

Table 3. Water chemistry parameters from discrete water samples collected at the study sites during CAU recovery. DIC: dissolved inorganic carbon.

Archipelago	Island/Atoll	Site	Chl-a (μg/L)	PO_4^{3-} (μM)	$Si(OH)^{4-}$ (μM)	NO_3^- (μM)	NO_2^- (μM)	NO_3^-+NO_2 (μM)	DIC	Total Alkalinity	Salinity
Pacific	Baker	**BAK02**	0.099	0.119	1.092	0.286	0.030	0.316	1914.632	2256.760	34.393
Remote		**BAK11**	0.142	0.143	1.008	0.289	0.037	0.326	1912.032	2246.860	34.229
Island		**BAK14**	0.052	0.178	1.142	0.270	0.036	0.306	1899.453	2237.490	34.198
Areas		**BAK16**	0.118	0.176	1.148	0.134	0.031	0.165	1907.366	2243.360	34.215
	Howland	**HOW05**	0.061	0.225	1.152	0.234	0.040	0.273	1923.141	2251.400	34.243
		HOW11	0.057	0.261	1.168	0.311	0.044	0.355	1919.946	2255.880	34.330
		HOW12	0.047	0.194	1.147	0.175	0.028	0.203	1907.032	2250.920	34.262
		HOW13	0.052	0.170	1.088	0.129	0.028	0.157	1904.506	2247.430	34.250
	Jarvis	**JAR01**	0.128	0.381	1.247	3.457	0.176	3.633	2020.984	2329.840	35.477
		JAR08	0.085	0.399	1.862	3.895	0.186	4.081	2021.194	2326.440	35.444
		JAR10	0.099	0.373	1.306	3.658	0.172	3.830	2018.226	2325.900	35.471
		JAR11	0.085	0.441	2.163	4.335	0.167	4.502	2024.863	2324.820	35.441
	Johnston	**JOH09**	0.198	0.835	1.069	0.281	0.056	0.338	1960.300	2257.980	35.186
		JOH10	0.080	0.193	0.915	0.164	0.018	0.182	1984.282	2304.380	35.076
		JOH11	0.047	0.159	0.895	2.406	0.057	2.462	1987.198	2303.430	35.058
	Kingman	**KIN03**	0.128	0.281	1.304	1.751	0.099	1.850	1949.211	2259.080	34.841
		KIN04	0.425	0.226	1.167	0.652	0.071	0.723	1964.640	2285.170	34.806
		KIN05	0.345	0.254	1.061	1.265	0.074	1.339	1966.420	2264.910	34.822
		KIN07	0.146	0.340	1.381	2.112	0.098	2.210	1969.447	2261.740	34.805
		KIN10	0.104	0.316	1.362	2.299	0.090	2.389	1967.024	2251.430	34.816
		KIN11	0.146	0.240	1.240	1.008	0.081	1.089	1963.311	2281.420	34.810
		KIN13	0.113	0.305	1.329	1.646	0.141	1.788	1971.513	2276.060	34.840
		KIN16	0.065	0.248	1.219	1.050	0.101	1.151	1956.153	2276.403	34.815
	Palmyra	**PAL01**	0.132	0.254	1.207	2.157	0.176	2.333	1997.999	2285.630	34.893
		PAL05	0.179	0.318	0.967	1.912	0.161	2.073	1972.856	2289.030	34.928
		PAL11	0.071	0.323	1.367	3.520	0.122	3.642	1953.555	2249.800	34.793
		PAL12	0.189	0.318	1.137	1.976	0.168	2.144	1976.987	2288.100	34.926
		PAL19	0.137	0.338	1.065	2.363	0.185	2.548	1980.134	2287.060	34.938
		PAL21	0.217	0.313	1.054	1.983	0.164	2.147	1973.778	2289.080	34.924
		PAL25	0.061	0.274	1.331	2.559	0.202	2.761	1978.131	2283.410	34.933
		PAL26	0.189	0.271	1.524	2.147	0.160	2.308	1982.910	2284.640	34.927
American	Ofu-	**OFU01**	0.028	0.174	0.987	0.686	0.026	0.711	1980.514	2326.340	35.548
Samoa	Olosega	**OFU02**	0.090	0.193	0.964	0.703	0.021	0.724	1993.481	2342.730	35.671
		OFU03	0.104	0.196	0.954	0.323	0.016	0.339	1988.740	2322.960	35.507
		OFU04	0.061	0.178	0.908	0.609	0.022	0.631	1983.488	2337.600	35.661
		OFU06	0.085	0.227	1.039	0.441	0.022	0.463	2000.860	2347.800	35.722
		OFU09	0.038	0.165	0.939	0.201	0.020	0.221	1982.082	2337.270	35.554
		OLO01	0.104	0.211	0.835	0.642	0.027	0.669	1980.276	2320.360	35.461
		OLO04	0.033	0.162	1.017	0.176	0.012	0.188	1980.092	2338.080	35.637
		OLO05	**0.043**	**0.168**	0.969	0.455	0.022	0.477	1987.800	2321.530	35.540
	Rose	**ROS01**	0.024	0.143	1.381	0.734	0.055	0.789	1989.284	2351.650	35.821
		ROS03	0.024	0.160	0.982	1.248	0.054	1.302	1997.380	2353.190	35.832
		ROS04	0.038	0.213	0.855	0.501	0.023	0.525	1998.827	2352.570	35.824

(*Continued*)

Table 3. (*Continued*)

Archipelago	Island/Atoll	Site	Chl-a (μg/L)	PO_4^{3-} (μM)	$Si(OH)^{4-}$ (μM)	NO_3^- (μM)	NO_2^- (μM)	NO_3^-+NO_2 (μM)	DIC	Total Alkalinity	Salinity
		ROS06	0.033	0.159	0.952	0.660	0.022	0.682	1991.501	2357.540	35.824
		ROS07	0.057	0.165	0.930	1.013	0.038	1.051	1993.537	2351.890	35.797
		ROS08	0.274	0.173	0.568	0.009	0.007	0.016	1992.341	2345.350	35.813
		ROS09	0.387	0.179	0.682	0.030	0.021	0.052	1995.747	2350.240	35.808
		ROS19	0.024	0.127	0.960	0.607	0.020	0.626	1990.731	2356.380	35.830
		ROS23	0.043	0.235	0.997	0.505	0.022	0.527	1995.147	2350.060	35.830
		ROS25	0.043	0.185	0.927	0.830	0.056	0.886	1993.840	2338.330	35.800
	Swains	**SWA01**	0.057	0.171	0.916	0.442	0.025	0.466	1976.990	2324.600	35.377
		SWA03	0.047	0.157	0.893	0.419	0.029	0.448	1985.097	2315.480	35.380
		SWA07	0.024	0.131	0.883	0.193	0.016	0.209	1966.418	2325.240	35.359
		SWA08	0.043	0.110	0.503	0.173	0.013	0.187	1965.466	2321.030	35.359
		SWA16	0.031	0.163	0.866	0.464	0.029	0.493	1983.123	2320.943	35.421
	Tau	**TAU02**	0.033	0.178	1.797	0.203	0.012	0.215	2002.217	2345.500	35.587
		TAU04	0.047	0.148	1.026	0.157	0.008	0.165	2004.007	2334.260	35.632
		TAU07	0.033	0.164	0.900	0.216	0.013	0.229	1977.969	2332.520	35.484
		TAU08	0.033	0.174	2.514	0.215	0.010	0.226	1979.494	2337.970	35.559
		TAU09	0.090	0.154	1.775	0.158	0.015	0.173	1997.330	2355.710	35.784
		TAU11	0.061	0.179	0.981	0.245	0.012	0.257	1984.880	2342.220	35.598
		TAU12	0.099	0.265	1.094	0.323	0.020	0.343	2004.229	2352.890	35.868
	Tutuila	**TUT01**	0.250	0.191	1.244	0.463	0.043	0.506	1981.687	2309.060	35.419
		TUT02	0.397	0.196	1.149	0.118	0.022	0.140	1983.039	2334.540	35.455
		TUT05	0.151	0.157	1.083	0.480	0.035	0.515	1967.571	2314.790	35.371
		TUT06	0.076	0.217	1.177	1.202	0.072	1.274	1988.110	2309.950	35.385
		TUT08	0.118	0.228	1.399	0.492	0.041	0.533	1982.673	2313.040	35.291
		TUT09	0.179	0.203	1.276	0.193	0.033	0.226	1965.812	2322.180	35.477
		TUT10	0.231	0.221	1.547	0.693	0.052	0.745	1976.364	2314.330	35.423
		TUT13	0.189	0.171	1.412	0.377	0.031	0.408	1967.817	2314.630	35.246
		TUT14	0.146	0.171	1.221	0.534	0.042	0.577	1978.316	2312.230	35.346
		TUT16	0.090	0.140	0.909	0.501	0.027	0.528	1977.106	2328.470	35.461
		TUT17	0.113	0.166	0.710	0.563	0.025	0.588	1968.627	2318.640	35.419
		TUT19	0.179	0.179	1.275	0.498	0.030	0.528	1962.147	2310.270	35.267
		TUT22	0.156	0.211	1.147	0.341	0.026	0.367	2011.997	2344.960	35.738

doi:10.1371/journal.pone.0142196.t003

perfect match; values closer to zero indicate little to no overall similarity between the two data sets [59, 60]. Prior to analysis, raw percent cover data were consolidated into functional groups [i.e., biofilm, scleractinian coral, calcified invertebrates (excluding scleractinian coral), fleshy invertebrates, CCA, fleshy encrusting macroalgae, calcified encrusting macroalgae (excluding CCA), fleshy upright macroalgae, calcified upright macroalgae (excluding *Halimeda*), *Halimeda*, turf algae, empty CAU tile, unidentifiable $CaCO_3$, loose sediment; (Table 2)]; analyses were limited to sites having both LPI and CAU cover data sets (see Table 1). Data from CAUs was averaged by site (n = 4 or 5) and utilized structural composition data from the top plate only. Both the LPI and CAU data were square root-transformed to reduce the influence of abundant functional groups and increase the influence of less common groups, and resemblance matrices were created using Bray-Curtis similarity. The RELATE test was used on the LPI and CAU data matrices based on Spearman rank correlation method with 9,999 permutations. A result rho-value (ρ) close to 1 would indicate high similarity in patterns of ranked order abundance between the LPI and CAU matrices, while a value close to zero would indicate little similarity.

Results

Accretion rates

Of the 390 CAUs deployed, 365 were recovered (94%); missing CAUs occurred haphazardly across a variety of sites including forereef, lagoon, sheltered, and exposed sites. Rose Atoll and Ta`u had the highest percentage of missing CAUs, with 10 and 15% of units missing, respectively. Net accretion rates varied across a wide range of spatial and environmental constructs including reef zone (forereef vs. lagoon), latitude, island, exposure (leeward vs. windward), population (urban settlements vs. none), geomorphology (carbonate vs. volcanic), and sites (Fig 3). Individual CAU accretion rates varied by orders of magnitude; they ranged from 0.004 g $CaCO_3$ cm^{-2} yr^{-1} at JOH-10, a lagoon site at Johnston Atoll, to 0.251 g $CaCO_3$ cm^{-2} yr^{-1} at JAR-01 on the forereef at Jarvis Island. Of the 78 sites examined, average accretion rates differed between islands (n = 11) and reef zones (forereef vs. lagoon). There was no interaction, but each factor had a significant main effect, with rates being significantly greater at forereef sites compared to lagoon sites (Fig 4A and 4B) (two-way ANOVA; $F_{ISLAND} = 16.19$, $df = 10$, $p<0.001$; $F_{REEF\ ZONE} = 33.13$, $df = 1$, $p<0.01$) (Table 4). Differences among islands exhibited a spatial pattern according to latitude; the equatorial reef systems at Howland, Baker, Jarvis, Palmyra, and Kingman Reef exhibited comparable accretion rates, with no statistical differences among them. Contrastingly, significantly different levels of variability were evident among the higher-latitude reef systems, with Tutuila exhibiting the lowest rates and Rose Atoll the highest ($p<0.001$, Tukey pairwise multiple comparison); no differences were evident between Swains, Ta`u, and Ofu-Olosega ($p>0.05$, Tukey pairwise multiple comparison). $CaCO_3$ accretion rates at these higher-latitude islands (Ofu-Olosega, Ta`u, and Swains) did not differ from the equatorial reef systems above mentioned ($p>0.05$, Tukey pairwise multiple comparison). In addition, urbanization and human inhabitation did not have a clear effect on the inter-island patterns of $CaCO_3$ accretion. Although Johnston Atoll, Palmyra Atoll, and Tutuila exhibited the lowest island/atoll-wide accretion rates and coincidentally have undergone the greatest levels of human disturbance (extensive dredging, morphological changes, deforestation, land-based sources of pollution, and nuclear and biological weapons testing), the pattern of inhabitation/high disturbance regime and low accretion rates was not consistent for other inhabited islands such as Swains, Ta`u and Ofu-Olosega or historically human impacted reef systems such as those at Howland, Baker, and Jarvis. This is likely due to the low levels of human inhabitation at Swains, Ta`u and Ofu-Olosega (population = 17, 790, and 358, respectively) (U.S. Census Bureau 2010[61]. Considering forereef sites only, accretion rates differed significantly

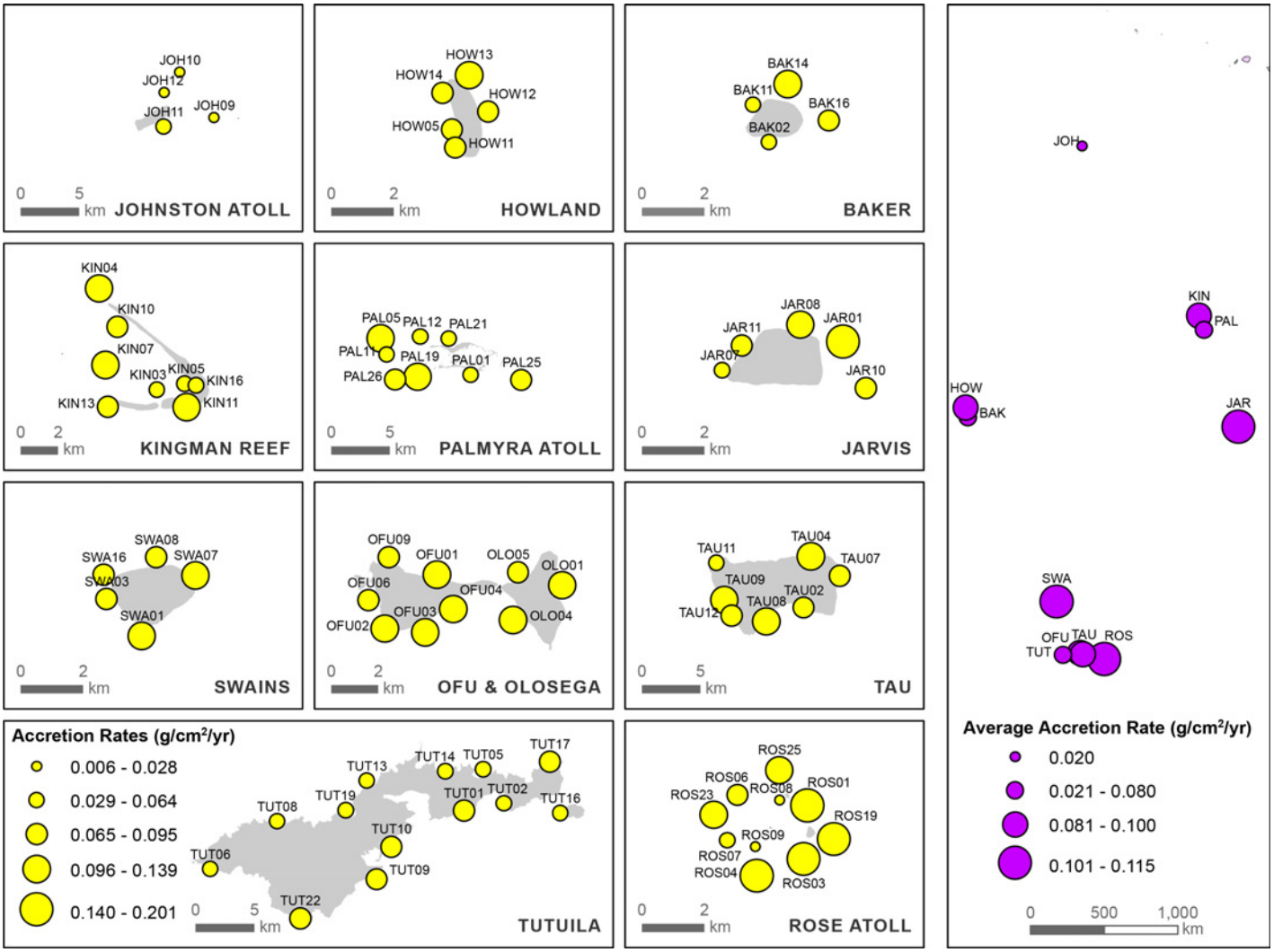

Fig 3. Spatial distribution and mean carbonate accretion rates derived from CAU deployments by study site (left panel) and island-wide (right panel).

doi:10.1371/journal.pone.0142196.g003

among islands and levels of wave exposure (leeward vs. windward), but no interaction effects among factors were detected, with rates being significantly greater at windward sites compared to leeward sites (Fig 4C and 4D) (two-way ANOVA; $F_{ISLAND} = 14.18$, $df = 10$, $p<0.001$; $F_{EXPOSURE} = 4.91$, $df = 1$, $p = 0.027$) (Table 4). For the main effect of islands and exposure, this difference was only statistically significant at equatorial and topographic-upwelling islands of Baker, and Jarvis. Finally, the third two-way ANOVA using island geomorphology (volcanic vs. carbonate) and exposure (leeward vs. windward) revealed a significant interaction between these factors (two-way ANOVA; $F_{EXPOSURE \times GEOMORPH} = 9.66$, $df = 1,1$; $P = 0.002$) (Table 4). At carbonate islands, accretion was higher at windward compared to leeward sites, but rates were equivalent at both exposures on volcanic islands (Fig 4E).

Community composition and percent cover

Mean island-wide percent cover of the major calcifying organisms on the reef benthos and those that recruited to the top surface of upper CAU plates are contrasted in Fig 5. Overall, the

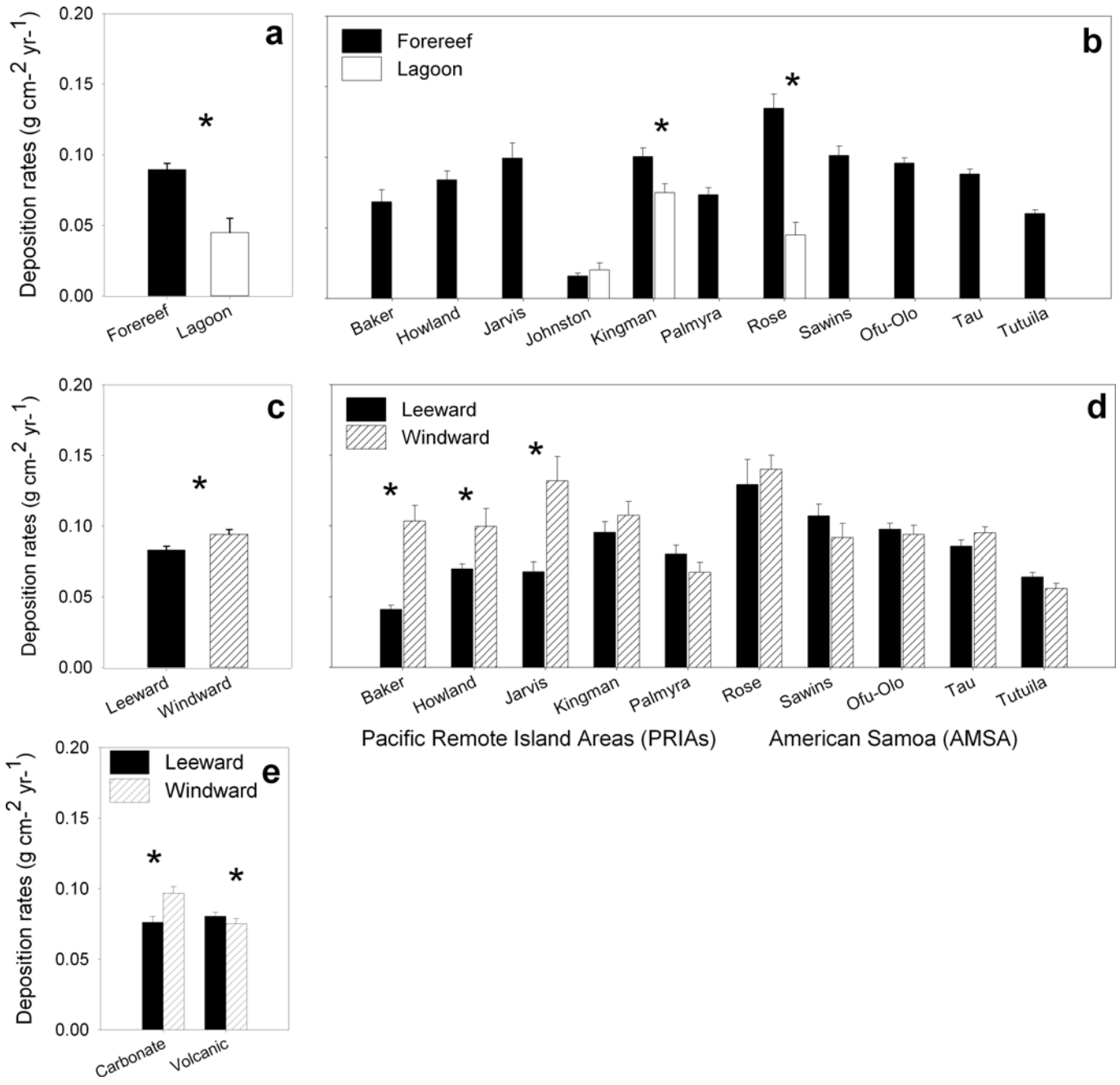

Fig 4. Graphic representation of the independent ANOVA model results illustrating the spatial variation patterns in net $CaCO_3$ accretion rates among island and reef zones (a, b); islands and levels of wave exposure (c, d), and island geomorphology (volcanic vs. carbonate) and wave exposure (e). Islands graphed in order of latitude; asterisks indicate significant differences among bar pairs.

doi:10.1371/journal.pone.0142196.g004

percent cover of calcifying to non-calcifying taxa differed between the CAU plates and the benthos (78.4% ± 2.2 and 68.7% ± 1.8, respectively; Kruskal-Wallis ANOVA, $\chi^2 = 13.31$, $df = 1$, $p<0.001$) (Table 4), as well as the proportion of cover represented by each of the different calcifying functional groups. For example, for all sites combined, CAUs were dominated by CCA (66%), with a lesser contribution by $CaCO_3$ sediment (4.4%), and calcified algal crusts (4.1%). This contrasts with the benthic communities at the deployment sites, where the major

Table 4. Summary results (F, χ^2, R, and P values) of all independent ANOVA and correlation statistical tests run to analyze accretion, percent cover, and water chemistry data.

Test	F	χ^2	R	P
Two-way ANOVA: Mean net accretion rates				
Island	16.19			< 0.001
Reef zone	33.13			< 0.001
Island x Reef zone		No interaction effects		
Island	14.18			< 0.001
Exposure	4.91			0.027
Island x Exposure		No interaction effects		
Exposure	0.49			0.48
Geomorphology	3.02			0.08
Exposure x Geomorphology	9.66			0.002
Kruskal-Wallis ANOVA				
Mean % cover of calcifiers (CAU vs. benthos)		13.31		<0.001
Mean % CCA cover on CAUs/Islands		97.97		< 0.001
Mean % Turf + macroalgal cover on CAUs/Islands		44.42		< 0.001
Spearman Rank Order Correlations				
Mean % CCA cover on CAUs vs. accretion rates			0.64	< 0.001
Mean % CCA cover on benthos vs. accretion rates			0.42	< 0.001
Mean % CCA cover on CAUs vs. benthos			0.44	<0.001
Island mean accretion rates vs. TA			0.30	<0.01
Island mean accretion rates vs. Chl-a			-0.47	<0.001
Island mean accretion rates vs. PO_4^{3-}			-0.13	>0.05
Island mean accretion rates vs. $Si(OH)^{4-}$			0.03	>0.05
Island mean accretion rates vs. NO_3^-			0.10	>0.05
Island mean accretion rates vs. NO_2^-			0.22	>0.05
Island mean accretion rates vs. NO_3^-+NO_2^-			0.10	>0.05
Island mean accretion rates vs. DIC			0.21	>0.05
Island mean accretion rates vs. Salinity			0.29	0.01

doi:10.1371/journal.pone.0142196.t004

calcifying taxa included scleractinian corals (32%), CCA (26%), and calcified algae (6% predominantly *Halimeda* and Peyssonneliales). For all reef systems with the exception of Johnston Atoll, CCA represented more than 50% of cover on the CAU plates and differences in CCA cover among islands were statistically significant (Kruskal-Wallis ANOVA, $\chi^2 = 97.97$, $df = 10$, $p<0.001$) (Table 4). Interestingly, the community composition on the CAU plates for Johnston and Tutuila exhibited a greater proportion of fleshy macroalgae and turf algae combined (Mean ± SE: 25.1% ± 6.1; 16.1% ± 2.9, respectively), compared to the other islands and atolls (7.1% ± 0.9), and those differences were statistically significant (Kruskal-Wallis ANOVA, $\chi^2 = 44.42$, $df = 10$, $p<0.001$; Dunn's Test pairwise multiple comparisons) (Table 4).

Biotic and abiotic correlates

Percent cover of CCA on CAUs was significantly correlated with net accretion rates ($r = 0.64$, $p<0.001$; Spearman Rank Order Correlation), as was CCA cover of the benthos ($r = 0.42$, $p<0.001$; Spearman Rank Order Correlation) (Table 4). Despite a significant association between percent cover of CCA on the CAU plates and the benthos ($r = 0.44$, Spearman rank order correlation) the RELATE analysis indicated that overall benthic communities found on CAU plates did not closely resemble what was found on the surrounding substrate, this was

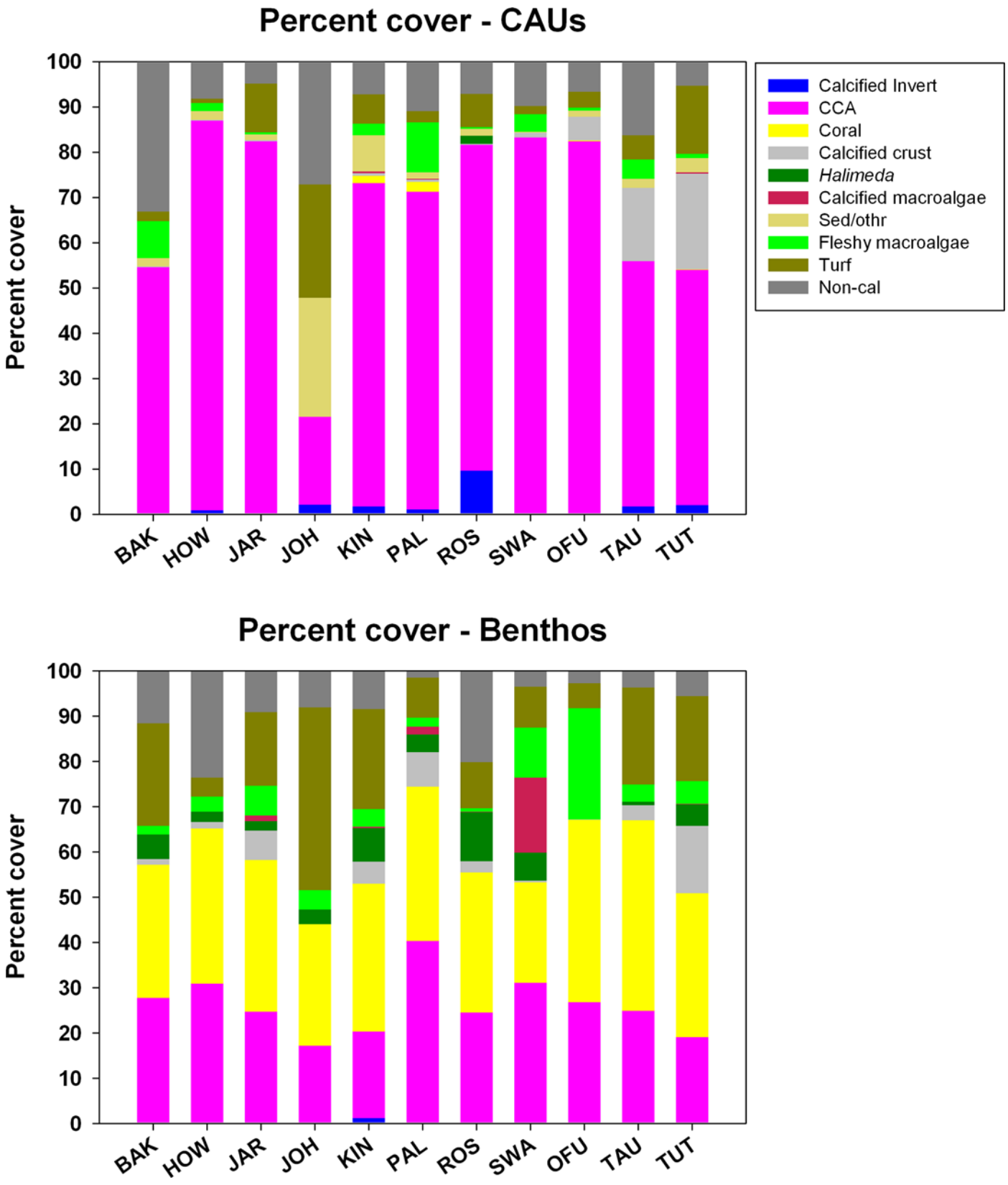
Percent cover - CAUs
Percent cover
100
90
80
70
60
50
40
30
20
10
0
BAK
HOW
JAR
JOH
KIN
PAL
ROS
SWA
OFU
TAU
TUT
Calcified Invert
CCA
Coral
Calcified crust
Halimeda
Calcified macroalgae
Sed/othr
Fleshy macroalgae
Turf
Non-cal
Percent cover - Benthos
Percent cover
100
90
80
70
60
50
40
30
20
10
0
BAK
HOW
JAR
JOH
KIN
PAL
ROS
SWA
OFU
TAU
TUT

Fig 5. Percent cover of the upper CAU plate and the surrounding site benthos derived from image analysis and LPI surveys (see methods for details) and classified by functional groups: Calcified invertebrate; CCA: crustose coralline algae; coral; calcified algal crusts; *Halimeda*; calcified macroalgae; sediments/other; fleshy macroalgae; turf; and non-calcified material. BAK: Baker Island; HOW: Howland Island, JAR: Jarvis Island; JOH: Johnston Atoll; KIN: Kingman Reef; PAL: Palmyra Atoll; ROS: Rose Atoll; SWA: Swains Island; OFU: Ofu and Olosega Islands; TAU: Ta`u Island; and TUT: Tutuila Island.

doi:10.1371/journal.pone.0142196.g005

clearly evient from the low rho-value ($\rho = 0.243$). We also found a positive statistical association between mean accretion of CCA and *in situ* total alkalinity and salinity ($r = 0.30$, $p<0.001$ and $r = 0.29$, $p = 0.01$, respectively; Spearman Rank Order Correlation), and a negative statistical association with chlorophyll-*a* concentration ($r = -0.47$, $p<0.001$; Spearman Rank Order Correlation); mean Island accretion rates exhibited non-significant correlations all the other water chemistry parameters (Table 4).

The optimal abiotic REVS model corroborated the results from the independent correlation tests above. As such, the spatial variability in the carbonate accretion rates on forereefs was best explained by two environmental predictor variables: total alkalinity and chlorophyll-a ($r = 0.33$, $p = 0.0079$ and $r = -0.4$, $p = 0.001$, respectively; REVS). In the subsequent GAM analysis, only total alkalinity was retained as the explanatory variable. For the lagoon sites, the optimal abiotic REVS model contained two environmental predictor variables that were positively associated with the carbonate accretion rates: silicon hydroxide (dissolved silica; $r = 0.77$, $p = 0.0095$) and dissolved inorganic carbon ($r = 0.82$, $p = 0.0041$). In the subsequent GAM analysis, only dissolved silica was retained as a statistically significant predictor variable. The biotic variables to best predict the spatial variation in carbonate accretion rates on forereefs included CCA cover and coral cover ($r = 0.54$, $p<0.001$; $r = -0.03$, $p = 0.824$, respectively; REVS) however, due to the low level of association only CCA was retained as statistically significant predictor in the GAM analysis. Finally, for the lagoon sites, the optimal biotic REVS model identified four explanatory variables; two were positively correlated with carbonate accretion rates [*Halimeda* ($r = 0.69$, $p = 0.0197$) and non-coralline encrusting macroalgae ($r = 0.15$, $p = 0.6583$)] and two were negatively correlated turf algae ($r = -0.47$, $p = 0.1456$) and fleshy upright macroalgae ($r = -0.48$, $p = 0.1329$)]. Of these, *Halimeda* was the only statistically significant variable retained in the GAM analysis.

Carbonate mineralogy

When net site-specific accretion rates were combined with the percent cover of the different functional groups of known mineralogy recruited to the CAUs and on the benthos, high Mg-calcite was found to be the dominant carbonate polymorph of the reef early successional stages. For oceanic reef systems such as Howland, Baker, Jarvis, Johnston, Swains, Rose, and Palmyra, the net accretion of organisms depositing high Mg-calcite represented over 70% on the CAU plates, compared to ~30% on the benthos (Fig 6). These differences are to be expected, given that CCA was the major calcifying functional group recruiting to the CAU plates, in contrast to the reef benthos where organisms depositing aragonite (scleractinian corals, milleporids, and *Halimeda*) out-weighed those depositing high Mg-calcite.

Discussion

This study presents a comprehensive, quantitative assessment of the rates of net $CaCO_3$ accretion *in situ* across a diverse range of reef systems in the central and south Pacific and demonstrates that: 1) net carbonate accretion rates of early reef successional stages varied considerably across a wide range of spatial and environmental constructs, including island, site, reef zone, latitude, exposure (leeward vs. windward), population (urban settlements vs.

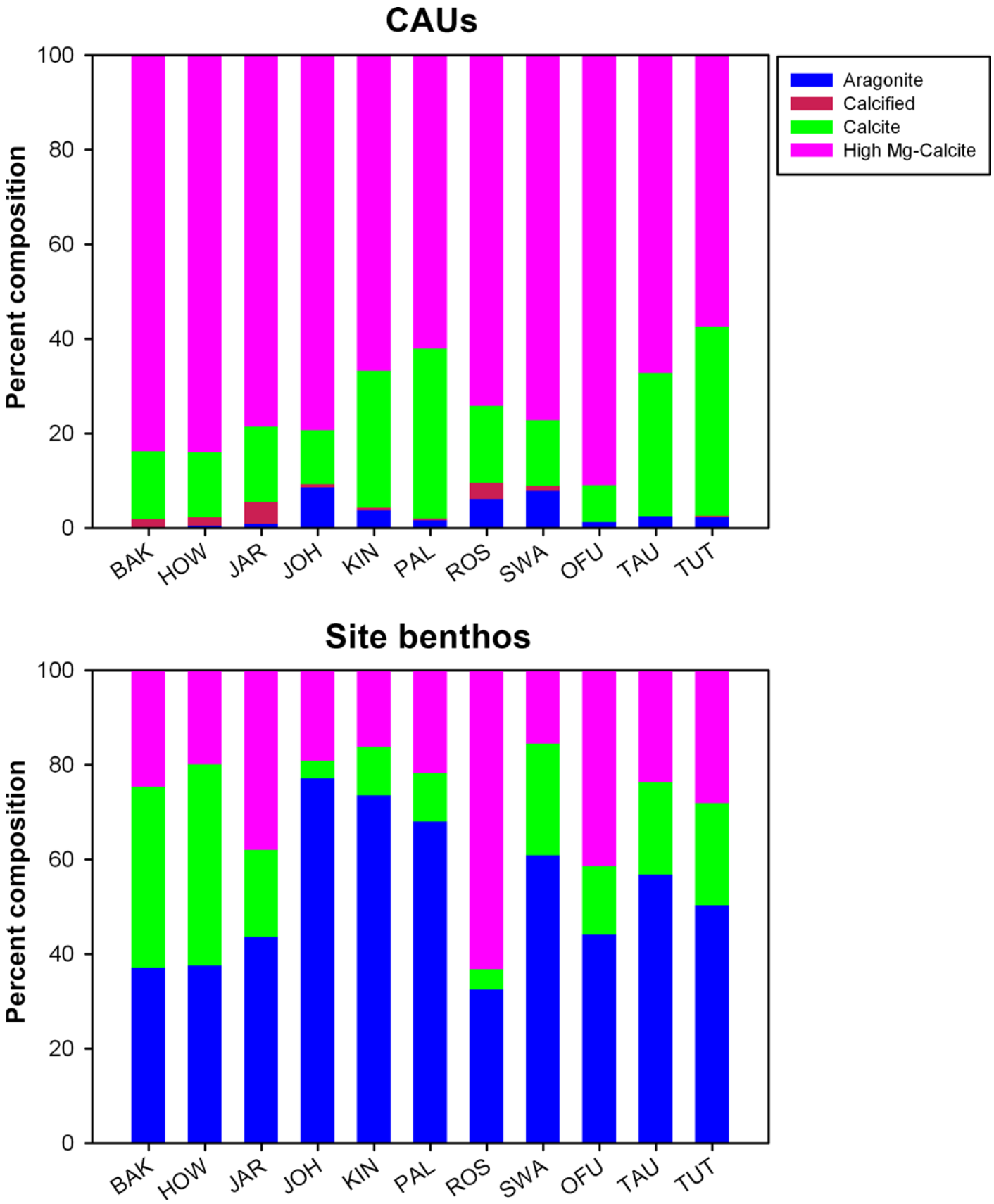
CAUs
Percent composition
100
80
60
40
20
0
Aragonite
Calcified
Calcite
High Mg-Calcite
BAK
HOW
JAR
JOH
KIN
PAL
ROS
SWA
OFU
TAU
TUT
Site benthos
Percent composition
100
80
60
40
20
0
BAK
HOW
JAR
JOH
KIN
PAL
ROS
SWA
OFU
TAU
TUT

Fig 6. Percent composition of the various $CaCO_3$ polymorphs computed based on the in-situ percent cover of the different functional groups recruited to the CAU plates and on the mature benthos (see methods for details). Calcified: unidentified calcified material. BAK: Baker Island; HOW: Howland Island, JAR: Jarvis Island; JOH: Johnston Atoll; KIN: Kingman Reef; PAL: Palmyra Atoll; ROS: Rose Atoll; SWA: Swains Island; OFU: Ofu and Olosega Islands; TAU: Ta`u Island; TUT: Tutuila Island.

doi:10.1371/journal.pone.0142196.g006

none), and geomorphology (volcanic vs. carbonate); 2) CCA benthic percent cover of the surrounding benthos, total alkalinity, and chlorophyll-a concentrations were significant predictor variables for net carbonate accretion rates on forereef habitats, and dissolved silica and percent cover of *Halimeda* were the significant predictor variable for lagoon habitats, respectively; and 3) the composition and relative abundance of the key early successional taxa recruited on to CAUs differed from that of the surrounding, mature benthos, with the former being overwhelmingly dominated by crustose coralline algae (CCA; >70% cover). The results of this study also provide insight into $CaCO_3$ accretion rates on standardized surfaces across an anthropogenic gradient, from relatively undisturbed, quasi-pristine coral reefs to human impacted (see [62]).

The large range of accretion rates within and among islands are likely the result of the complex and spatially variable nature of the physical and biological processes driving the structure and function of reef communities. Overall, accretion rates were higher on forereef sites than in lagoon habitats because of the higher amount of CCA present on CAUs from these reef zones. Although the lagoon environments at Johnston, Rose, and Kingman Reef are very different from each other, the observed forereef vs. lagoon differences are likely driven by key coral reef community structural determinants, including depth, light availability, wave exposure, as well as, the disparate levels of water circulation and flushing, turbidity and sedimentation, and productivity that characterize each reef zone [63, 64, 65]. The effect of exposure (leeward vs. windward), was only manifest for the three equatorial islands in the PRIA (Baker, Howland, and Jarvis). This difference is at least partially due to the intense topographic upwelling of the Equatorial Undercurrent on the west side of all three equatorial islands; upwelling brings more nutrients, reduced light penetration, and sedimentation of organic particles [50]. CCA are photosynthetic organisms that require adequate light levels to calcify and grow; in addition high phosphate concentrations have been demonstrated to be detrimental to CCA development [66]. Moreover, the leeward environs on the three equatorial islands above-mentioned are characterized by steep-sloping forereefs compared to the windward facing habitats which are typified by broad shallow, forereef terraces [65, 67]. Shading on the steep leeward reef slope could also contribute to lower levels of carbonate accretion for these areas, whereas reef communities on the broad shallow forereef terraces of windward shores received full sun exposure.

With the exception of Palmyra Atoll, the equatorial reef systems at Howland, Baker, Jarvis, and Kingman, exhibited comparable net carbonate accretion rates. In contrast, carbonate accretion rates in American Samoa and Johnston Atoll exhibited notably high levels of variability. Johnston and Tutuila at 16°N and 14°S, respectively, had the lowest average accretion rates (0.019 g $CaCO_3$ cm^{-2} yr^{-1} and 0.060 g $CaCO_3$ cm^{-2} yr^{-1}, respectively) and Rose Atoll the highest (14°S, 0.116 g $CaCO_3$ cm^{-2} yr^{-1}); accretion rates for the islands of Swains, Ta`u, and Ofu-Olosega were comparable to each other (0.09–0.100 g $CaCO_3$ cm^{-2} yr^{-1}). Interestingly, the three reef systems exhibiting the lowest average accretion rates (i.e., Johnston Atoll, Palmyra Atoll, and Tutuila) have also, historically, experienced the highest levels of human impact. For example, Johnston and Palmyra atolls were extensively dredged and substantially modified to accommodate the operation of military naval bases and air strips during the WWII U.S. Pacific campaign. Some of these alterations resulted in widespread, chronic changes to water clarity and circulation, in addition to more recent human disturbances including localized iron-leaching from ship groundings and PCB contamination [67].

For Tutuila, increasing anthropogenic impacts resulting from significant human inhabitation and subsequent urban development have degraded water quality in many reef habitats around the island, particularly due to runoff carrying considerable amounts of sediments and nutrients [68]. Higher nutrient levels facilitate the proliferation of fast-growing macroalgae and turf algae, which in turn can easily out-compete reef calcifiers for space and resources. Concomitantly, increased runoff generally results in reductions in water clarity, which in turn can negatively affect the net carbonate accretion rates, given that the main reef calcifiers are photosynthetic and require clean, well-lit waters [69,70]. Overfishing of reef herbivores, particularly parrotfish and surgeonfish, is an additional result of increasing population pressure at Tutuila [68]. With the loss of grazers, epiphytic filamentous and turf algae can quickly overgrow reef calcifiers and these effects are often exacerbated when increased nutrients are implicated [71]. As such, the combined effects of chronic human disturbances together with decreased pH from ocean acidification will likely affect reef community structure and therefore carbonate accretion on coral reefs worldwide [72].

The spatial variability in CAU net accretion rates at forereef sites was related to total alkalinity (TA). TA, defined as the stoichiometric sum of the bases in solution, is a measure of the capacity of water to resist changes in pH. In tropical reef ecosystems TA is predominantly governed by the concentration of the carbonate ion (CO_3^{2-}) in seawater; benthic and water-column processes, including biological calcification and photosynthesis can drive site-level changes in carbonate ion concentrations [47, 73, 74]. As such, a positive, statistical association between TA and net accretion rates is expected because higher pH and TA conditions shift the carbonate system balance to thermodynamically favor $CaCO_3$ precipitation. In addition, Chl-a concentration was the optimal biotic predictor variable of net accretion rates at forereef sites. As previously mentioned, high nutrient concentrations, in particularly phosphate, have a detrimental effect of CCA calcification and growth [66]. Because Chl-a concentration is a proxy for ocean photosynthetic productivity, which in turn is affected by nutrient availability [50], a negative statistical association with accretion rates would be expected. The significant association between accretion rates and percent CCA benthic cover is also expected given that CCA was the overall greatest contributor to $CaCO_3$ accretion rates of early reef successional stages.

For the lagoon sites, two environmental variables were positively correlated with the carbonate accretion rates: dissolved silica and dissolved inorganic carbon (DIC), of which only dissolved silica was retained in the GAM analysis as a significant predictor variable. This finding is consistent with the selection of percent *Halimeda* benthic cover as the sole biotic predictor variable that correlated significantly and positively with carbonate accretion rates. Although *Halimeda* is one of the major carbonate producers in tropical reef systems [32], it was rare or completely absent from all the lagoon sites at Rose and Johnston atolls, and only moderately high at two outer lagoon sites at Kingman Reef. The statistical associations between the predictor variables and the carbonate accretion reflect the pattern of relatively high accretion rates at the two lagoon sites at Kingman reef (KIN-07 and KIN-10) and substantially low accretion rates at the remaining lagoon sites (Fig 3). While the intrinsic drivers of these associations remain unclear, we suggest that the low sample size (n = 10) in concert with the marked structural and ecological differences between the three lagoon systems (e.g., open lagoons at Kingman and Johnston vs. closed lagoon at Rose Atoll; relatively pristine conditions at Rose Atoll and Kingman Reef vs. extensive anthropogenic impacts at Johnston Atoll) may be in part implicated in the spatial patterns reported herein; further study is recommended.

The average percent cover of the main benthic components at the study sites was approximately: 33% for scleractinian corals, 26% for CCA, and 16% for turf algae; on the CAU plates these taxa represented 0.4%, 70%, and 7%, respectively. It is the disparate proportions in percent cover of the key early successional taxa on CAU plates and the mature benthos the main

reason why the RELATE analysis showed little similarity between CAU plates and the surrounding benthos. This can be explained in part due to the short deployment period (2 years) of the experimental units. Nonetheless, despite those differences, the spatial variability in carbonate accretion rates reported in this study could be predicted by the combination of biotic and abiotic parameters, demonstrating the utility of CAUs as a monitoring tool for the effects of ocean acidification (OA).

In addition, high Mg-calcite was found to be the dominant carbonate polymorph deposited on the CAU plates. This is expected, given that CCA was the major calcifying functional group recruiting to the CAU plates, in contrast to the reef benthos where organisms depositing aragonite (scleractinian corals, milleporids, and *Halimeda*) out-weighed those depositing high Mg-calcite. Many coralline algal species precipitate high Mg-calcite [75], with the highest molar mass of $MgCO_3$ ratio at low latitudes and warm temperatures [11]. High Mg-calcite is the most soluble form of biogenic $CaCO_3$, making coralline algae amongst the most susceptible coral reef taxa to ocean acidification [21, 45].

A great deal of emphasis has been devoted to understanding and characterizing the effects of OA on tropical coral reef ecosystems [76]. Nonetheless, despite their pivotal role as major source of reef limestone, reef habitat creation, and their association with the recruitment process of key reef elements including scleractinian corals, insufficient attention has been paid to the potential implications of elevated ocean pCO_2 to crustose coralline algae [36, 77, 78]. With CCA representing such an important proportion of calcifying biota both on the early reef successional community, as well as the mature reef benthic community, it is clear that the effects of OA can profoundly affect coral reef function at multiple ecological levels: from the recruitment of CCA and the organisms dependent on them for settlement [37], to the production, stabilization, and cementation of the reef framework and carbonate sediments [79, 80].

Our study provides insight into variation in carbonate accretion rates, primarily by CCA, at dozens of sites across the central and south Pacific, and offers a unique perspective to contextualize our comprehension of the effects of OA at different scenarios of future ocean chemistry. As such, three main inferences can be gleaned from our observations: (1) the spatially variable nature of the accretion rates reported herein suggest that reef community responses will likely vary widely between reef systems, but between sites within islands as well; (2) because CCA precipitate a highly soluble polymorph of $CaCO_3$, changes in ocean water acidity will likely result in lower CCA accretion rates; and (3) under acidified conditions CCA may lose their competitive advantage as the dominant calcifying taxa of the early reef successional community, which in turn may have adverse implications for the settlement and development of other important reef calcifying taxa. Therefore, under the projected changes in marine seawater carbonate chemistry, the ability of marine biomineralizers to cope with such changes and continue offering the ecosystem services they currently provide will likely be determined by both the magnitude and rate of seawater pH decrease. As such, the combined effects of chronic human disturbances together with decreased pH from ocean acidification will likely affect reef community structure and therefore carbonate accretion on coral reefs worldwide

Acknowledgments

This work was supported by the NOAA Ocean Acidification Program and the NOAA NMFS Office of Science and Technology. Institutional, logistic, and financial support was also provided by NOAA Pacific Islands Fisheries Science Center's Coral Reef Ecosystem Division (CRED) and Scripps Institution of Oceanography. Permission to work in American Samoa and the Pacific Island National Marine Monument was granted by the American Samoa Department of Marine and Wildlife Resources, the National Park of American Samoa, the National

Marine Sanctuary of American Samoa, and by the U.S. Fish and Wildlife Service. Thanks are due to the officers and crew of the NOAA Ship *Hi'ialakai* for support with dive and small boat operations. A number of CRED staff assisted with construction, deployment, and recovery of the CAU assemblies. E Penland, E Looney, P Misa-Lozada, B Richards, and H, Bailey assisted with CAU lab processing; staff from J Smith Lab at Scripps helped with the CAU plate image analysis, and T Acoba, J Ehses, and A Dillon assisted with figure preparation and formatting. The authors also want to thank B Schumacher, J Samson, P Misa-Lozada, and T Oliver, as well as to anonymous reviewers, whose comments greatly improved this manuscript. The manuscript contents are solely the opinion of the authors and do not constitute a statement of policy, decision, or position on behalf of NOAA or the U.S. Government.

Author Contributions

Conceived and designed the experiments: REB NNP JS CWY. Performed the experiments: CWY CLR. Analyzed the data: BVA PSV CLR NNP TS MDJ. Contributed reagents/materials/analysis tools: JS. Wrote the paper: BVA CLR PSV NNP TS MDJ REB.

References

1. Ulfsbo A. The marine carbonate system: ionic interactions and biogeochemical processes. PhD thesis, University of Gothenburg; 2014. 88 pp.
2. Erez J, Reynaud S, Silverman J, Schneider K, Allemand D. Coral calcification under ocean acidification and global change. In: Dubinsky Z, Stambler N, editors. Coral reefs; an ecosystem in transition. Ney York, Springer Press; 2011. pp. 151–176.
3. Sabine CL, Feely RA, Gruber N, Key RM, Lee K, Bullister JL, et al. The Oceanic sink for anthropogenic CO2. Science. 2004; 305(5682): 367–371, doi: 10.1126/science.1097403 PMID: 15256665
4. Tanhua T, Bates NR, Körtzinger A. The Marine Carbon Cycle and Ocean Carbon Inventories. In: Siedler G, Griffies S, Gould J, and Church J, editors. Ocean Circulation and Climate, International Geophysics Series 103. Academic Press, Oxford; 2013. pp. 787–815.
5. Fabricius K, De'ath G, Noonan S, Uthicke S. Ecological effects of ocean acidification and habitat complexity on reef-associated macroinvertebrate communities. Proc. R. Soc. B. 2013; 282: 20132479.
6. Solomon S, Qin D, Manning M, Chen Z, Marquis M, Averyt KB, et al. Climate Change 2007: The Physical Science Basis: Contribution of Working Group I to the Fourth Assessment Report of the Intergovernmental Panel on Climate Change. Cambridge Univ. Press; 2007.
7. Feely RA, Doney CL, Cooley SR. Ocean acidification: present conditions and future changes in a high-CO2 world. Oceanography. 2009; 22: 37–47.
8. Fearnside PM. Global warming and tropical land-use change: Greenhouse gas emissions from biomass burning, decomposition and soils in forest conversion, shifting cultivation and secondary vegetation. Climatic Change. 2000; 46 (1–2): 115–158.
9. IPCC. Climate Change 2013: The Physical Science Basis. Contribution of Working Group I to the Fifth Assessment Report of the Intergovernmental Panel on Climate Change. In: Stocker TF, Qin D, Plattner GK, Tignor M, Allen SK, Boschung J, et al. editors. Cambridge University Press, Cambridge; 2013. 1535 pp, doi: 10.1017/CBO9781107415324
10. Houghton JT, Meira Filho LG, Callander BH, Harris N, Kattenberg A, Maskell K, et al Climate change 1995: The science of climate change. Cambridge Univ. Press, Cambridge; 1996.
11. Meehl GA, Stocker TF, Collins WD, Friedlingstein P, Armandou T, Gaye AT, et al. Climate change 2007: The physical science basis: contribution working group 1, 4th assessment report of the Intergovernmental Panel in Climate Change. In: Solomon S, Qun D, Manning M, Chen A, Marquis M, Averyt KB, et al. editors. Climate Change. Cambridge University Press, Cambridge, UK; 2008. pp. 747–845.
12. Smith JB, Schneider SH, Oppenheimer M, Yohe GW, Hare W, Mastrandrea MD, et al. Assessing dangerous climate change through an update of the Intergovernmental Panel on Climate Change (IPCC) "reasons for concern". Proc. Natl. Acad. Sci. 2009; 106: 4133–37. doi: 10.1073/pnas.0812355106 PMID: 19251662
13. Orr JC, Fabry VJ, Aumont O, Bopp L, Doney SC, Feely RA, et al. Anthropogenic ocean acidification over the twenty-first century and its impact on calcifying organisms. Nature. 2005; 437:681–686. PMID: 16193043

14. Hoffman GE, Barry JP, Edmunds PJ, Gates RD, Hutchings DA, Klinger T, et al. The effect of ocean acidification on calcifying organisms in marine ecosystems: and organism to ecosystem perspective. Ann. Rev. Ecol. Sys. 2010; 41: 127–47.
15. Andersson AJ, Mackenzie FT, Bates NR. Life on the margin: implications of ocean acidification on Mg-calcite, high latitude and cold-water marine calcifiers. Mar. Ecol. Prog. Ser. 2008; 373:265–273.
16. Cooley SR, Doney SC. Anticipating ocean acidification's economic consequences for commercial fisheries. Environmental Research Letters. 2009; 4: 8 pp.
17. Cooley SR, Kite-Powell HL, Doney SC. Ocean acidification's potential to alter global marine ecosystem services. Oceanography. 2009; 22 (4):172–181.
18. Dufault AM, Cumbo VR, Fan T, Edmunds PJ. Effects of diurnally oscillating pCO2 on the calcification and survival of coral recruits. Proceedings of the Royal Society Biological Sciences. 2012; 279 (1740):2951–2958. doi: 10.1098/rspb.2011.2545 PMID: 22513858
19. Kurihara H, Matsui M, Furukawa H, Hayashi M, Ishimatsu A. Long-term effects of predicted future seawater CO2 conditions on the survival and growth of the marine shrimp *Palemon pacificus*. J. Exp. Mar. Biol. Ecol. 2008; 367: 41–46.
20. Albright R, Langdon C. Ocean acidification impacts multiple early life history processes of the Caribbean coral *Porites astreoides*. Global Change Biology. 2011; 17: 2478–2487.
21. Jokiel PL, Rodgers KS, Kuffner IB, Andersson AJ, Cox EF, Mackenzie RT. Ocean acidification and calcifying reef organisms: a mesocosm investigation. Coral Reefs. 2008; 27:473–483.
22. Anthony KRN, Kleypas JA, Gattuso JP. Coral reefs modify their seawater carbon chemistry–implications for impacts of ocean acidification. Global Change Biology. 2011; 17: 3655–3666.
23. Crawley A, Kline d, Dunn S, Anthony K, Dove S. The effect of ocean acidification on symbiont photorespiration and productivity in *Acropora formosa*. Global Change Biol. 2010; 16: 851–63.
24. Fabry VJ, Seibel BA, Feely RA, Orr JC. Impacts of ocean acidification on marine fauna and ecosystem processes. ICES Journal of Marine Science. 2008; 65:414–432.
25. Pörtner HO, Langenbuch m, Michaelidis B. Synergistic effects of temperature extremes, hypoxia, and increases of CO2 on marine animals from Earth history to global change. J. Geophys. Res. 2005; 110: C09S10.
26. Kleypas JA, Buddemeier RW, Archer D, Gattuso JP, Langdon C, Opdyke BN. Geochemical consequences of increased atmospheric carbon dioxide on coral reefs. Science. 1999; 284:118–120. PMID: 10102806
27. Martin S, Gattuso JP. Response of Mediterranean coralline algae to ocean acidification and elevated temperature. Global Change Biology. 2009; 15:2089–2100.
28. Hoegh-Guldberg O, Bruno JF. The impacts of climate change on the word's marine ecosystems. Science. 2010; 328: 1523–1528. doi: 10.1126/science.1189930 PMID: 20558709
29. Price NN, Martz TR, Brainard RE, Smith JE. Dial variability in seawater pH relates to calcification and benthic community structure on coral reefs. PLoS ONE. 2012; 7(8): e43843. doi: 10.1371/journal.pone.0043843 PMID: 22952785
30. Anthony KRN, Kline DI, Diaz-Pulido G, Dove S, Hoegh-Gouldberg O. Ocean acidification causes bleaching and productivity loss in coral reef builders. Proc. Natl. Acad. Sci. 2008; 105: 17442–46. doi: 10.1073/pnas.0804478105 PMID: 18988740
31. Jokiel PL. Ocean acidification and control of reef coral calcification by boundary layer limitation of proton flux. Bull. Mar. Sci. 2011; 87: 633–657.
32. Price NN, Hamilton SL, Tootle JS, Smith JS. Species-specific consequences of ocean acidification for calcareous tropical green algae *Halimeda*. Mar. Ecol. Prog. 2011; Ser. 440: 67–78.
33. Comeau S, Edmunds PJ, Spindel NB, Carpenter RC. The responses of eight coral reef calcifiers to increasing partial pressure of CO2 do not exhibit a tipping point, Limnol. Oceanogr. 2013; 58: 388–398.
34. Lee D, Carpenter SJ. Isotopic disequilibrium in marine calcareous algae. Chem. Geol. 2001; 172: 307–329.
35. Vroom PS, Smith CM. The challenge of siphonous green algae. American Scientist. 2001; 89: 524–531.
36. Vroom PS, Smith CM. Life without cells. Biologist. 2003; 50: 222–226.
37. Diaz-Pulido G, McCook LJ, Larkum AWD, Lotze HK, Raven JA, Schaffelke B. Vulnerability of macroalgae of the Great Barrier Reef to climate change. In: Johnson J, Marshall P, editors. Climate change and the Great Barrier Reef. Great Barrier Reef Marine Park Authority and Australian Greenhouse Office, Australia; 2007. pp 151–192.
38. Nelson WA. Calcified macroalgae–critical to ecosystems and vulnerable to change: a review. Mar. Freshwater Res. 2009; 60: 787–801.

39. Price N. Habitat selection, facilitation, and biotic settlement cues affect distribution and performance of coral recruits in French Polynesia. Oecologia. 2010; 163: 747–758. doi: 10.1007/s00442-010-1578-4 PMID: 20169452

40. Heyward AJ, Negri AP. Natural inducers for coral larval metamorphosis. Coral Reefs. 1999; 18: 273–279.

41. Harrington L, Fabricius K, De'ath G, Negri A. Recognition and selection of settlement substrata determine port-settlement survival in corals. Ecology. 2004; 85: 3428–37.

42. Bosence DW. Coralline algal reef frameworks. J Geol Soc London. 1983; 140: 365–376.

43. Klumpp DW, McKinnon AD. Community structure, biomass and productivity of epilithic algal communities on the Great Barrier Reef: dynamics at different spatial scales. Mar. Ecol. Prog. 1992; Ser. 86: 77–89.

44. Adey WH. Coral reefs: algal structured and mediated ecosystems in shallow, turbulent, alkaline waters. Journal of Phycology. 1998; 34: 393–406.

45. Morse JW, Anderson AJ, Mackenzie FT. Initial responses of carbonate-rich sediments to rising atmospheric pCO2 and ocean acidification: role of high Mg-calcite. Geochimica et Cosmochimica Acta. 2006; 40: 5814–30.

46. Brinkman TJ, Smith AM. Effect of climate change on crustose coralline algae at a temperate vent site, White Island, New Zealand. Mar. Freshwater Res. 2015; 66: 360–370.

47. Semesi JS, Kahgwe J, Bjork M. Alterations in seawater pH and CO2 affect calcification and photosynthesis in the tropical coralline algal *Hydrolithon* sp (Rhodophyta). Estuar. Coast. Shelf Sci. 2009; 84: 337–341.

48. Kamenos NA, Burdett HL, Aloisio E, Findlay HS, Martin S, Longbone C, et al. Coralline algal structure is more sensitive to rate, rather than the magnitude, of ocean acidification. Global Change Biology. 2013; 19: 3621–3628. doi: 10.1111/gcb.12351 PMID: 23943376

49. Miller J, Maragos J, Brainard R, Asher J, Vargas-Ángel B, Kenyon J, et al. The State of Coral Reef Ecosystems of the Pacific Island Remote Areas. In: Waddell JE, Clarke AM, editors. The State of Coral Reef Ecosystems of the United States and Pacific Freely Associated States: 2008. NOAA Technical Memorandum NOS NCCOS 73. NOAA/NCCOS Center for Coastal Monitoring and Assessment's Biogeography Team. Silver Spring, MD; 2008. pp 353–386.

50. Gove JM, Williams GJ, McManus MA, Heron SF, Sandin SA, Vetter OJ, et al. Qualifying climatological ranges and anomalies for Pacific coral reef ecosystems. PLoS One 2013; 8(4):e61974. doi: 10.1371/journal.pone.0061974 PMID: 23637939

51. Sandin SA, Smith JE, Demartini EE, Dinsdale EA, Donner SD, Friedlander AM, et al. Baselines and degradation of coral reefs in the Northern Line Islands. PLoS ONE. 2008; e1548. doi: 10.1371/journal.pone.0001548 PMID: 18301734

52. Tucker ME, Wright VP. Carbonate sedimentology. Blackwell Scientific Publications, Oxford; 1990.

53. Smith AM, Sutherland JE, Kregting L, Farr TJ, Winter DJ. Phylomineralogy of the coralline red algae: correlation of skeletal mineralogy with molecular phylogeny. Phytochemistry. 2012; 81: 97–108. doi: 10.1016/j.phytochem.2012.06.003 PMID: 22795764

54. Goldberg W. The biology of reef organisms. University of Chicago Press, Chicago; 2013.

55. Preskitt LB, Vroom PS, Smith CM. A Rapid Ecological Assessment (REA) Quantitative Survey Method for Benthic Algae Using Photoquadrats with Scuba. Pacific Science. 2004; 58 (2): 201–209.

56. Dickson, AG, Sabine CL, Christian JR. Guide to best practices for ocean CO2 measurements. PICES Special Publication 3; 2007.

57. SYSTAT® SYSTAT 12 Statistics_I_II_III_IV. SYSTAT Software Inc., San Jose, California. 2007.

58. Goodenough AE, Hart AG, Stafford R. Regression with empirical variable selection: description of a new method and application to ecological datasets. PLoS ONE. 2012; 7(3): e34338. doi: 10.1371/journal.pone.0034338 PMID: 22479605

59. Clarke KR, Gorley RN. PRIMER v6: User Manual/Tutorial. PRIMER-E Plymouth; 2006. 190pp.

60. Clarke KR, Warwick RM. Change in marine communities: an approach to statistical analysis and interpretation, 2nd edition, PRIMER-E Plymouth; 2001.

61. US. Census Bureau. 2010 American Samoa Demographic Profile Data. Available: http://factfinder.census.gov/faces/tableservices/jsf/pages/productview.xhtml?pid=DEC_10_DPAS_ASDP1&prodType=table. Accessed 8 October 2015.

62. Vroom PS, Musburger CA, Cooper CW, Maragos JE, Page-Albins KN, Timmers MAV. Marine biological community baselines in unimpacted tropical ecosystems: Spatial and temporal analyses of reefs at Howland and Baker Islands. Biodivers. Conserv. 2010; doi: 10.1007/s10531-009-9735-y

63. Atkinson M, Grigg R. Model of a coral reef ecosystem. Coral Reefs. 1984; 3: 13–22.

64. Vecsei A. A new estimate of global reefal carbonate production including the fore-reefs. Global and Planetary Change. 2004; 43: 1–18.

65. Hamylton S, Pescud A, Leon J, Callaghan D. A geospatial assessment of the relationship between reef flat community carbonate production and wave energy. Coral Reefs. 2013; 32: 1025–1039.

66. Fabricius K, De'ath G. Environmental factors associated with the spatial distribution of crustose coralline algae on the Great Barrier Reef. Coral Reefs. 2001; 19:303–309.

67. Maragos J, Miller J, Gove J, DeMartini E, Friedlander AM, Godwin S, et al. U.S. coral reefs in the Line and Phoenix Islands, Central Pacific Ocean: history, geology, oceanography, and biology. In: Riegl B, Dodge RE, editors. Coral Reefs of the World Vol. I. Coral Reefs of the U.S.A. Springer Science + Business Media B.V. 2008. pp. 595–641.

68. Craig P, DiDonnato G, Fenner D, Hawkins C. The state of the coral reef ecosystems of American Samoa. In: Waddell J, editor. The state of the coral reef ecosystems of the United States and Pacific Freely Associated States: 2005. NOAA Technical Memorandum NOS NCCOS 11. NOAA/NCCOS Center for Coastal Monitoring and Assessment's Biogeography Team. Silver Spring, MS; 2005. pp. 312–337.

69. Borowitzka MA. Mechanisms of algal calcification. Prog. Phycol. Res. 1982; 1: 137–177.

70. Barnes DJ, Chalker BE. Calcification and photosynthesis on reef building corals and algae. In: Dubinsky Z, editor. Ecosystems of the world 25 Coral Reefs. Elsevier, Amsterdam; 1990. pp. 109–131.

71. Hallock P, Müller-Karger FP, Halas JC. Coral reef decline. Natl Geogr. Res. & Explor. 1997; 9: 358–378.

72. Silbiger NJ, Guadayol Ò, Thomas F, Donahue M. Reefs shift from net accretion to net erosion along a natural environmental gradient. Mar. Ecol. Prog. Ser. 2014; 515: 33–44.

73. Smith SV, Key GS. Carbon dioxide and metabolism in marine environments. Limnology and Oceanography. 1975; 20: 493–495.

74. Anthony KRN, Kleypas J, Gatuso JP. Coral reefs modify their seawater carbon chemistry–implications for impacts of ocean acidification. Global Change Biology. 2012; 17: 3655–3666.

75. Diaz-Pulido G, Nash MC, Anthony KRN, Bender D, Opdyke NB, Reyes-Nivia C, et al. Greenhouse conditions induce mineralogical changes and dolomite accumulation in coralline algae on tropical reefs. Nature Communications. 2014; 5:3310, doi: 10.1038/ncomms4310 PMID: 24518160

76. Noisette F, Duong G, Six C, Davoult D, Martin S. Effects of elevated pCO2 on the metabolism of a temperate rhodolith *Lithothamnion corallioides* grown under different temperatures. Journal of Phycology. 2013: 49: 746–757.

77. Kroeker KJ, Micheli F, Gambi MC. Martz TR. Divergent ecosystem responses within a benthic marine community to ocean acidification. Proc. Natl Acad. Sci. 2011; 108: 14515–14520. doi: 10.1073/pnas.1107789108 PMID: 21844331

78. Fabricius KF, Kluibenschedl A, Harrington L, Noonan, De'ath G. In situ changes of tropical crustose coralline algae along carbon dioxide gradients. Scientific Reports. 2015; 5: 9537, doi: 10.1038/srep09537 PMID: 25835382

79. Bosence DW. Coralline algal reef frameworks. J. Geol. Soc. London. 1983; 140:365–376.

80. Littler MM, Littler DS. Models of tropical reef biogenesis. Phycol. Res. 1984; 3:324–364.